Environ Earth Sci (2016)75:697
DOI 10.1007/s12665-016-5534-4

ORIGINAL ARTICLE

Geothermal energy potential of eastern desert region, Egypt

D. Chandrasekharam[1,2] · A. Lashin[3,4,5,6] · N. Al Arifi[2] · A. Al Bassam[2,6] · C. Varun[7] · H. K. Singh[1]

Received: 17 November 2015 / Accepted: 4 March 2016

Abstract Future energy security and CO_2 emissions investigation models indicate that the best option for Egypt is to adopt a mitigation strategy by using geothermal energy as an energy source mix and implement energy efficiency policy. The hydrothermal potential is estimated to be of the order of 158×10^6 kWh while El Faliq high heat-generating granite has the potential to generate billion kWh of electricity. Through these two geothermal energy sources, the country can mitigate CO_2 reduction to the order of 20 million tones and provide sustained freshwater to domestic, agricultural and industrial sectors. Egypt in future may have to address two important issues such as guaranteed future electricity supply and freshwater supply to meet the growing population and agriculture demand. The current situation indicates that the Nile River may not be able to sustain the demand due to uncertainties in the monsoon pattern and reduction in storage capacity. A renewable energy (geothermal) source mix and implementing a sound energy efficient policy in agricultural, transport and domestic sectors will help the country to meet the future food and water demand of the country.

Keywords Egypt · EGS · Geothermal · Desalination · Red Sea

Introduction

It has been reported that Egypt has embarked on a vision to encourage and support renewable energy-related industries in the Middle East and North Africa (MENA) mainly to address issues related to environment resulting due to large CO_2 emissions. The region west of Suez Gulf is the prime area of focus for investors in wind energy that is estimated to generate 20,000 MW of installed capacity. Similarly, solar photovoltaic (solar PV)-based power is estimated at 74,000 TWh/year (Khalil et al. 2010). In the rural areas, biomass is the main source of energy and in conjunction with the solid waste the biomass resources are estimated to generate 20 MTOE/year. What is not realized is the available geothermal resources that also form a part of renewable energy that are located along the eastern desert region adjacent to the Red Sea. The geothermal energy in combination with other renewables motioned above can change the socio-economic status of the rural population and support the future population with energy and food security. Although the oil and gas resources of Egypt is supporting the current energy demand, CO_2 emissions from power, industrial and transport sectors are causing anomalous changes in the microenvironmental systems that is influencing the global climate system. The geothermal

✉ D. Chandrasekharam
dchandra50@gmail.com

1 Department of Earth Sciences, Indian Institute of Technology Bombay, Mumbai 400076, India

2 Geology and Geophysics Department, College of Science, King Saud University, Riyadh 11451, Saudi Arabia

3 Geology Department, Faculty of Science, Benha University, Benha 13518, Egypt

4 Petroleum and Natural Gas Engineering Department, College of Engineering, King Saud University, Riyadh 11421, Saudi Arabia

5 Geothermal Resources Engineering Group, Sustainable Energy Technologies Centre, King Saud University, Riyadh, Saudi Arabia

6 Saudi Geological Survey (SGS) Research Chair, King Saud University, Riyadh, Saudi Arabia

7 GeoSyndicate Power Pvt. Ltd., Mumbai, India

Published online: 12 April 2016

resources in the eastern desert region are represented in the form of hydrothermal and enhanced geothermal systems (EGS) within the radiogenic granites. This paper aims at describing the geothermal energy (EGS) potential of the eastern desert region and its contribution in supporting sustainable development of rural areas by providing energy and water security.

Present energy demand and CO_2 emissions

Egypt is the oil-rich North African country with 2152 billion cubic metres of remaining gas reserves and ranks seventh among the non-OPEC countries. The country still has 566 billion cubic metres of undiscovered natural gas (de la Vega 2010). The country is planning to expand its exploration programme to enhance gas exports from the current 17 billion cubic metres to 23 billion cubic metres by 2030. But, within the country the energy demand is increasing rapidly due to population growth, industrial and transportation sectors growth (de la Vega 2010). This demand will be at its peak when Egypt's population crosses 100,000 by 2030 from the present 80,000. The country needs to find alternate energy source mix to support its demand and increase its oil exports as planned. In a recent report, de la Vega (2010) analysed Egypt's energy demand under three scenarios: (1) business as usual scenario (BAU) where the gross domestic product (GDP) is expected to grow at 3.1 % until 2030. In this scenario, the country has no concern for the CO_2 emissions. (2) High economic growth (HEG) scenario where the growth is expected at 4.5 %. The CO_2 emissions in this scenario will be higher than the BAU scenario because of higher consumption of power from the existing power plants supported by fossil fuels. This growth scenario is detrimental to the country in future and will have higher impact on the global climate change. (3) Substitution and efficiency scenario (S&E) renewables and energy efficiency play an important role in controlling CO_2 emissions and sustaining satisfactory growth and GDP only after 2020. These three scenarios are shown in Fig. 1.

Substantial emissions reduction can be achieved under S&E scenario only by the residential sector (Fig. 2) while the industrial and transport sector may not contribute much to CO_2 reduction under this sector (Chandrasekharam et al. 2016).

The oil consumption by the domestic sector in 2030 under S&E scenario is about 20,000 million tonnes less compared to present-day consumption due to the proposed energy efficiency measures adopted by Egypt and contributions from renewables (Chandrasekharam et al. 2016). The three scenarios analysed by de la Vega (2010) are based on solar PV, wind and biofuels substituting the fossil fuels-based energy sources. However, Egypt has substantial quantity of geothermal resources that have not been taken into account (Chandrasekharam et al. 2015). The

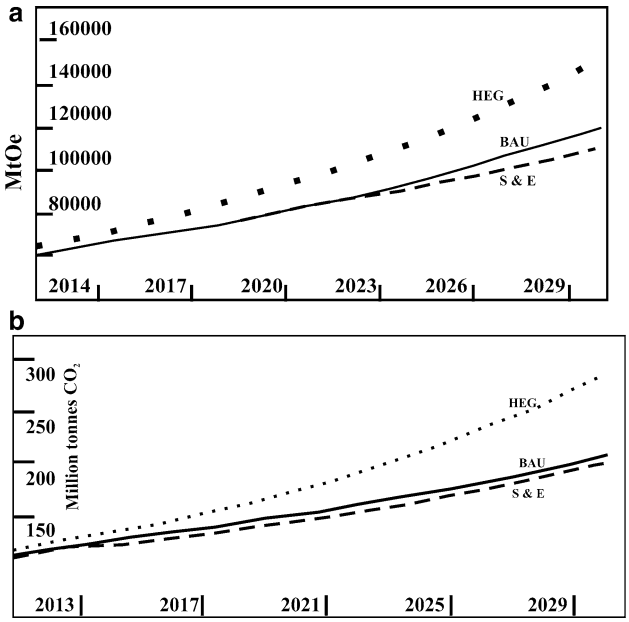

Fig. 1 Energy consumption and CO_2 emissions under the three scenarios (modified after de la Vega 2010)

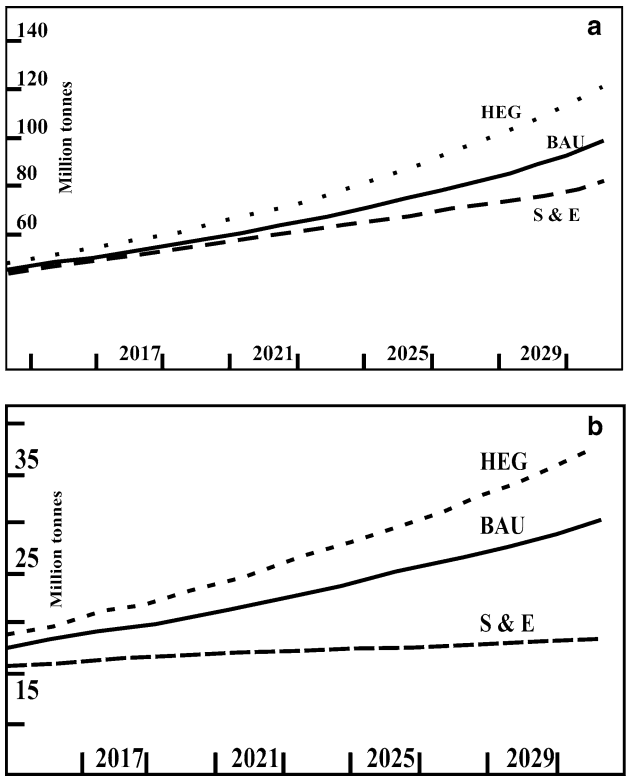

Fig. 2 CO_2 emissions by **a** transport and **b** residential sectors under the three scenarios

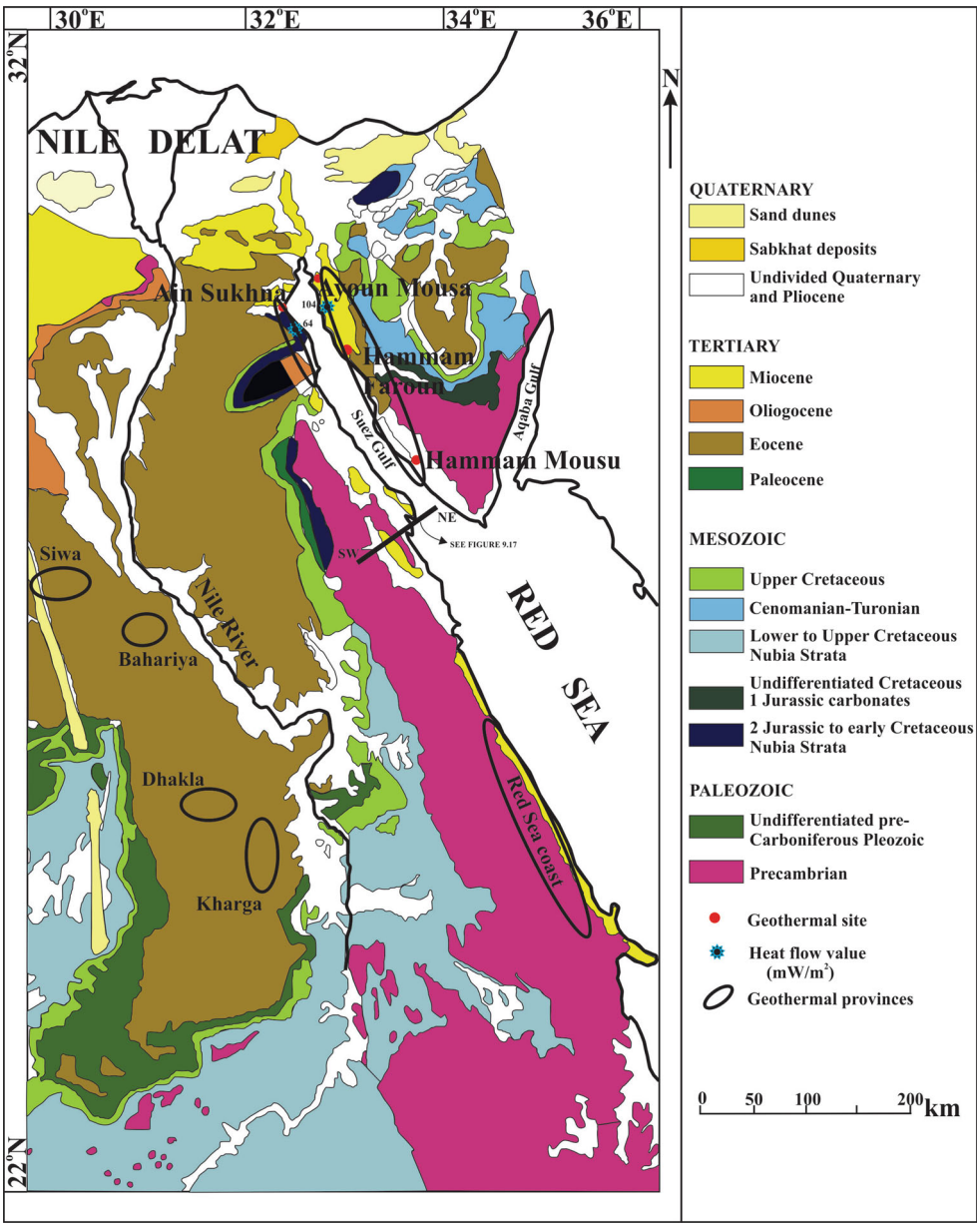

Fig. 3 Geological and structural map of Egypt showing the geothermal provinces (modified after Chandrasekharam et al. 2015)

geothermal resources are represented by hydrothermal systems around the Gulf of Suez and EGS represented by high heat-generating rock of granitic composition in the eastern desert region that are discussed in the following sections.

Geological and tectonic setting

The Gulf of Suez is considered as the failed arm of the Red Sea rift that was initiated near the Afar junction and propagated north between Oligocene and Early Miocene (Colletta et al. 1988; Patton et al. 1994; Zaher et al. 2011). The Red Sea rift truncated the Nubian–Arabian shield into the Nubian and Arabian shields. A major part of the Nubian shield is located in the eastern desert region along the western margin of the Red Sea and southern part of the Sinai desert (Fig. 3).

The Nubian–Arabian shield was formed under an island arc accretion tectonic environment between 800 and 600 Ma (Stern 1985, 1994; Stern and Johnson 2010). The Nubian shield forms the basement over which the subsequent formations that are present on the eastern margin of Red Sea are deposited in this region (Fig. 3). Extensional rift tectonics within the Gulf of Suez, resulting from the active Red Sea rifting, gave rise to several horst and graben structure along the western and eastern side of the Suez Gulf and along the eastern desert adjoining the western Red

Sea margin. Early regional tectonic regime in Egypt is represented by two mega lineaments that cut across the African continent and truncate towards the Red Sea in Egypt. The Precambrian shield is transacted by the Trans-African Lineament (TAL) and the Central African Lineament (CAL), the two regional mega lineament extending from Cameroon and Central Africa, respectively (Nagy et al. 1976; Schandelmeier and Pudlo 1990; El Ahmady Ibrahim et al. 2015). These two regional mega lineaments host alkaline granite plutons and its equivalents. They are highly sheared and hence are silicified and kaolinized. These silicified and kaolinized granites are rich in rare earth elements (REE and radioactive elements such as uranium, thorium and potassium (Eby 1992; Elsayed et al. 2014)). The thorium and uranium in these weathered and altered granite vary from 12 to 1100 and 13 to 300 ppm, respectively (Elsayed et al. 2014). In addition to the alkaline granites, the Precambrian basement is intruded by older (800–610 Ma) calc-alkaline granites and younger (530 Ma) alkaline granites that are also rich in uranium and thorium content.

In the eastern desert, older and younger granites outcrop. The older rocks of granitic composition, varying in age from 880 to 610 Ma, include diorite to tonalite, trondhjemite and monzonite and are deformed. In Egypt, the emplacement of these granites was related to Shaitian (850–800 Ma), Hafafit (760–710 Ma) and Meatiq (630 Ma) deformation phases (Lundmark et al. 2012; El Ramly and Akaad 1960; Bentor 1985; Hassan and Hashad 1990). The younger granites are the post-orogenic and syn-orogenic granites (600–530 Ma), and are alkaline to peralkaline in nature. These are the plutons that are emplaced in the older crust along the strike slip shear zones controlled by TAL and CAL (Stern et al. 1984; Fritz et al. 1996; Breger et al. 2002; Moussa et al. 2008; Lundmark et al. 2012). Like other countries around the Red Sea, Egypt also experienced volcanic activity between Jurassic–Early Cretaceous (Mesozoic volcanics; 155–125 Ma) and Late Cretaceous–Early Tertiary (90–60 Ma). They are exposed in the eastern and western deserts and Sinai (Fig. 3). The Cretaceous volcanic activity continued during Cenozoic and Palaeocene represented by pulses of volcanic activity. This is followed by wide spread tertiary basaltic volcanism that continued in Eocene. This episode is followed by volcanic activity related to the opening of the Red Sea (Perrin et al. 2009).

Geothermal manifestation

Geothermal springs are occur along the eastern and western margin of the Suez Gulf (at Hammam Faraun, Ayoun Mousa and Ain Sukhna) and at Kharga, Dhakla, Bahariya and Siwa (Fig. 3). Those thermal springs on either side of the Suez Canal are high-temperature springs (51–70 °C, Table 1) while those in other localities are warm springs with temperatures varying from 35 to 42 °C.

These sites registered high geothermal gradient and heat flow values that are far above the global values of 30 °C/km and 50 mW/m^2 as evident from the bottom hole temperatures recorded from oil wells around the geothermal sites on the west and eastern side of the Gulf of Suez. The temperatures vary from 120 to 260 °C, and heat flow is >95 mW/m^2 (Morgan et al. 1976; Zaher et al. 2011, 2012). Shallow geophysical investigation around these sites indicates deep circulation of meteoric water, within the fractured (high heat-generating) granites, as the source for the thermal springs in Hammam Faraun (Zaher et al. 2011; Abdalla, and Scheytt 2012).

The thermal waters are enriched in Cl^- ions and fall in the Na–Cl field in Fig. 4 (Piper 1953) but plot away from the Red Sea data. This shift appears to be due to large supply of $CaSO_4$ (see Table 1) from salt marshes present around the thermal spring sites and along the Red Sea coast (El Shaer 2010). The position of the cold spring in Fig. 4 suggests that this spring represents cooled thermal water emerging to the surface after a long near surface circulation. In the Giggenbach's Cl–SO_4–HCO_3 diagram (Fig. 5), the thermal springs plot towards the Cl apex but away from the mature—neutral water field of Giggenbach (1988) indicating involvement of high SO_4 water in modifying the chemistry of the thermal waters. The warm waters from oases clearly show mixing between the thermal and Nile River waters.

Table 1 Physical and chemical characteristics of cold and thermal waters and Red Sea, Egypt (modified after Chandrasekharam et al. 2015)

	Samp. no	Temp	Area	pH	Na^+	K^+	Ca^{++}	Mg^{++}	Cl^-	HCO_3^-	SO_4^-	Reff
1	Hammam Faroun 1	70	Egypt	6.5	4750	130	1039	489	9654	132	1450	7
2	Hammam Faroun 2	51	Egypt	7.1	4280	117	1039	422	8713	103	1450	7
3	Ayoun Mousa	37	Egypt	6.6	1794	60	594	267	3768	287	1250	7
4	Ain Sukhna	32	Egypt	7.6	1970	75.0	408	250	3730	207	1300	7
5	Nile R	28	Egypt	8.3	26	5.0	39	15	18	317	24	8
6	4G Spring	28	Egypt	8.0	520	5.0	270	110	1113	300	633	
7	Red Sea				92,850	1870	5150	764	155,500	143	840	

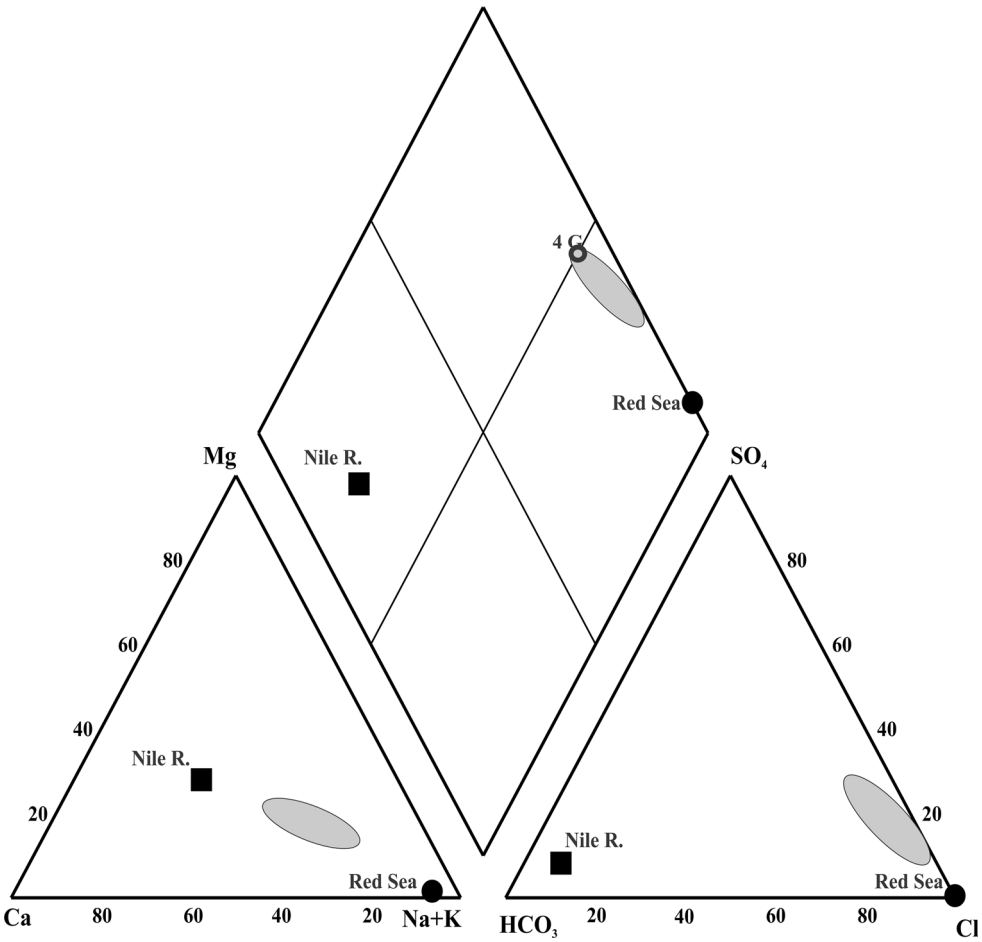

Fig. 4 Piper (1953) diagram showing the chemical characteristics of thermal and cold waters from Egypt

The position of the thermal waters in Figs. 4 and 5 may also indicate thermally heated waters from Sabkhas. But the fluoride content in the thermal waters (2–4 ppm, Swanberg et al. 1983) rules out this possibility and represents waters circulating within the high heat-generating granites rich in fluorite (Raslan and El-Feky 2012) in this region (Chandrasekharam et al. 2015; Lashin et al. 2014). Although the Suez Gulf thermal springs, due to their location within the high geothermal gradient and high heat flow value region, represent high-temperature reservoir conditions, due to this mixing with Sabkha waters, they slightly shift towards the lower end of the partially equilibrated waters in the Giggenbach's Na–K–Mg diagram (Fig. 6) giving a lower reservoir temperatures (120–160 °C).

EGS potential of Egypt

Radiogenic granites of the eastern desert

Granites and related intrusives with high radioactive element content are extensively found in the eastern desert, close to the Red Sea coast (Fig. 7, see "Present energy demand and CO_2 emissions") and are enriched in accessory minerals such as zircon, titanite, monazite, thorite and uranothorite. These late-stage granitic melts were enriched in uranium and thorium and have entered lattice of the late-stage crystallizing minerals such as fluorite. The uranium and thorium concentration in fluorites from granites varies from 2200 to 7500 ppm, respectively (Raslan and El-Feky 2012). High concentration of uranium and thorium is also reported in altered granites near Aswan city and close to Kukur and Dungul oases (Ibrahim et al. 2015). These granites are intruded into the 400 Ma sandstone and 216 Ma volcanic flows. The outcrop area of this granite is about 3 km^2 (Ibrahim et al. 2015) and a large part of the granite is covered by alluvium and Palaeozoic sandstone. Several basic dikes are seen cutting across the granites.

The most characteristic feature of the silicified and kaolinized granites, described earlier, is that they are enriched in uranium and thorium (Ibrahim et al. 2015). The concentration of uranium and thorium in silicified granites varies from 5 to 954 and 3–180 ppm, respectively. Similarly in the kaolinized granites, the uranium and thorium vary from 38 to 96 and 12–360 ppm, respectively (Ibrahim

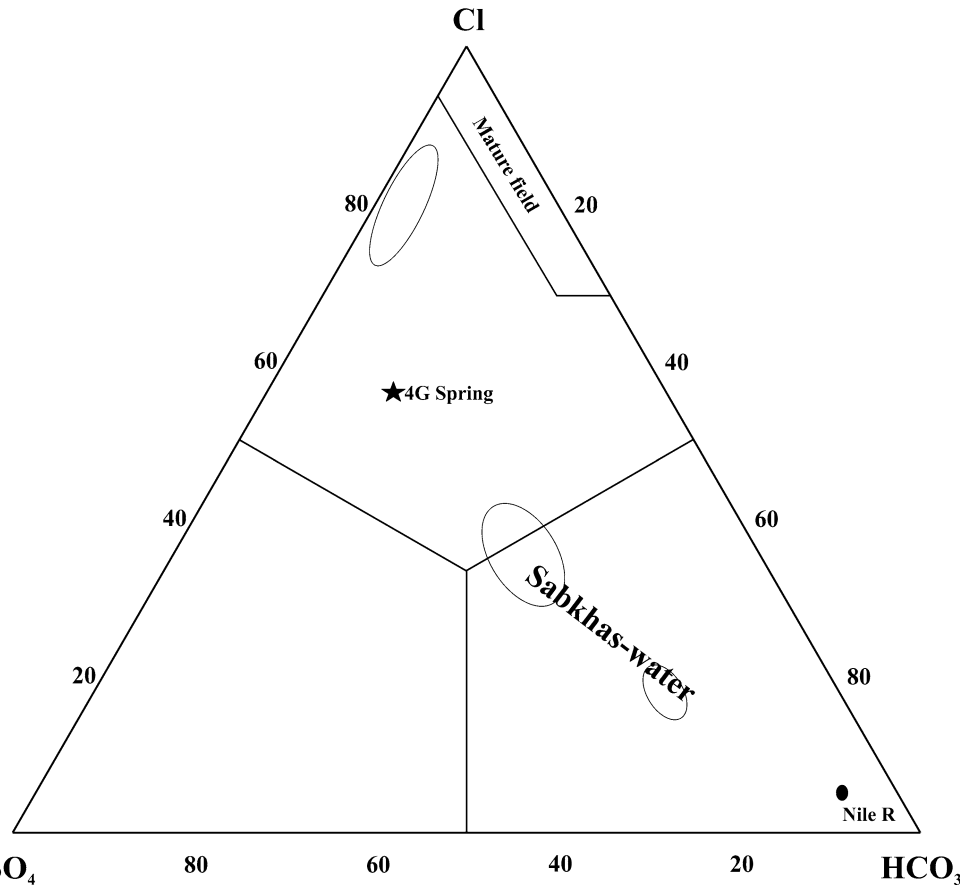

Fig. 5 Cl–SO_4–HCO_3 diagram of Giggenbach (1988) showing the chemical variation in the thermal waters, cold and Nile River waters

et al. 2015). In some cases, these granites host uranium mineralization of economic importance (Saleh et al. 2014; Emam et al. 2011; Saleh et al. 2006; Raslan and El-Feky 2012; Gaafar 2014). The concentration of uranium and thorium in these granites varies from 3047 to 6441 and 2383–1462 ppm, respectively (Lundmark et al. 2012). The uranium, thorium and potassium values in certain radiogenic granites and the heat generated by such granites are listed in Table 2.

Although the outcrop area for these granites is small, their roots have wider subsurface span occupying area of several square kilometres. On a regional scale, the Precambrian granites are insulated by a >600-m-thick sedimentary formation (Fig. 8) that contain (like a heat insulator) the heat that is generated by the granites and associated rocks as well as the heat conducted by the mantle through conduction. This feature is one of the most important factors for qualifying a site as a potential EGS site.

The radioactive heat production (RHP in mW/m^3) by these granites has been calculated using the heat generation constant (amount of heat released per gram of U, Th and K in per unit time) and the uranium, thorium and potassium concentrations C_U, C_{Th} and C_K (Table 2) using the equation suggested by Rybach (1976) and Cermak et al. (1982):

$$\mathrm{RHP} = \rho(9.52C_U + 2.56\,C_{Th} + 3.48\,C_K)\times 10^{-5}$$

where ρ is the density of rock in kg/m^3; C_U and C_{Th} are the concentration of U and Th in mg/kg, respectively, and C_K is the concentration of K in weight percentage in the granites. Th heat generation values by the granites over the western shield region are shown in Fig. 9 (values >5 mW/m^3 only are shown). The surface heat flow values were calculated using the method recommended by Lachenbruch (1968).

Heat flow values

Heat flow measurements from boreholes on either side of Suez Gulf and in the eastern desert regions have been reported by several authors (Evans and Tammemagi 1974; Girdler 1970, 1977; Gettings 1982; Gettings and Showail 1982; Morgan et al. 1977, 1981, 1983, 1985). The heat flow values measured over the sediments and granites and gneisses along the eastern desert are shown in Fig. 9 and the heat flow profile across the eastern desert extending from the Red Sea coast over a distance of about 200 km is also shown in Fig. 10. The heat flow values reported by Morgan et al. (1985) are low for the eastern desert region due to lack of large number of observation boreholes. For

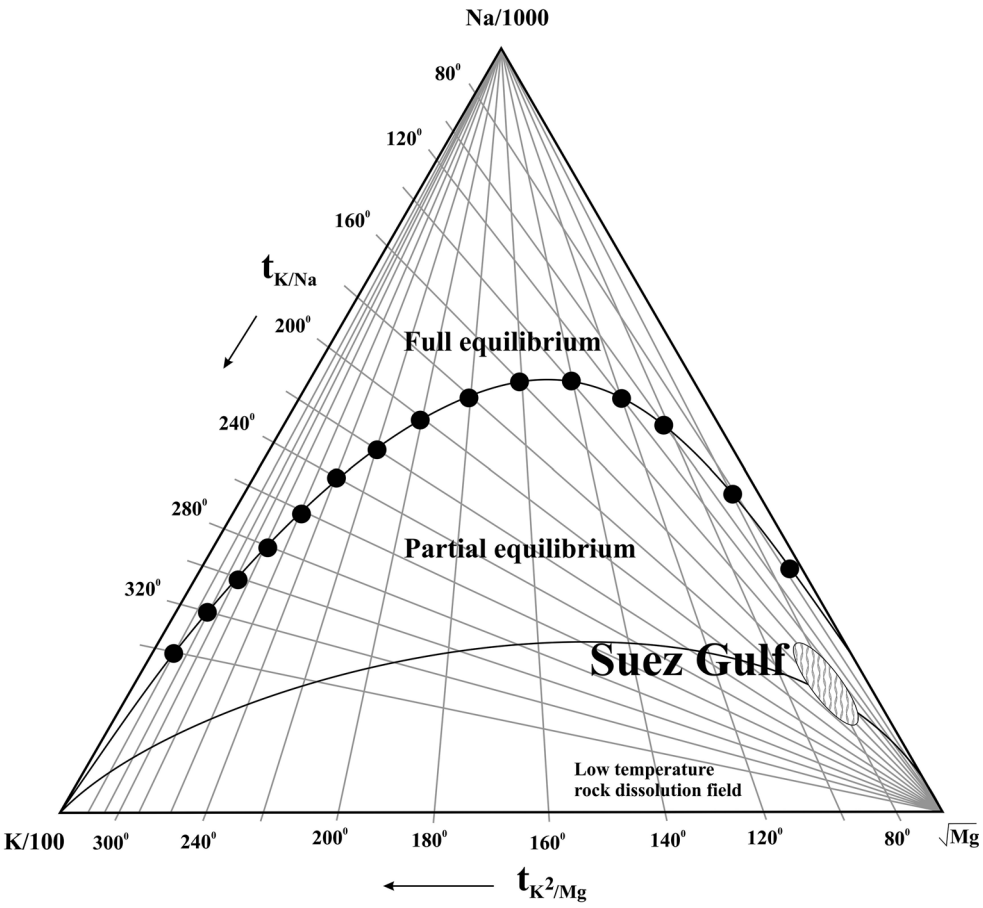

Fig. 6 Giggenbach K–Na–Mg diagram (Giggenbach 1988) indicating high reservoir temperatures for the Suez gulf thermal springs

example, the heat generated by the El Hidi granites, east of Aswan City, is about 107 mW/m^2 (Table 1) and high value is not reflected in the data published by the earlier authors while assessing the heat flow values of areas away from the Red Sea coast. The average heat generation by the granites is 18 μW/m^3, and the average heat flow value is 220 mW/m^2 (Table 2). This high value is apparently due to the occurrence of uranium-rich mineral phases and secondary uranium deposits in the younger granites and related rocks in the eastern desert. Thus, the thermal anomaly of the entire eastern desert is higher by several folds than that reported by earlier authors in Egypt (Figs. 9, 10) and also in regions adjacent to the Mediterranean Sea (e.g. Baba et al. 2008).

Thus, it is apparent that the granites and associated rocks occurring in Egypt in general and eastern desert region, in particular, are enriched in heat-generating radioactive elements and the heat generated by these granites is extremely high compared to normal granites. Granites of similar nature occur in the Arabian Shield, on the eastern side of the Red Sea (Chandrasekharam et al. 2015). Based on the heat flow values (Table 2), the subsurface temperature has been calculated using the following relation (Vernekar 1975)

$$Q = k(\mathrm{d}T/\mathrm{d}Z)$$

where k is the thermal conductivity of the rock and $\mathrm{d}T/\mathrm{d}Z$ is the thermal gradient. The subsurface temperature has been calculated by taking the average surface temperature as about 30 °C (Vernekar 1975) and thermal conductivity of the rock (i.e. granite with density of 2.75 g/cm^3) as 3.98 W m^{-1} C^{-1}. The estimated subsurface temperatures of the eastern desert region extending between the Red Sea coast and Nile River at 2 and 3 km depths have been calculated, and the results are shown in Fig. 11.

Discussion

Due to the scanty rainfall and large CO_2 emissions, Egypt and in fact all the countries around the Red Sea in general have two most important issues to address: (1) guaranteed future electricity supply to support the growing population, (2) freshwater to support growing demand in the domestic, agricultural and industrial sectors. The Nile River may not be able sustain the demand due to uncertainties in the monsoon pattern. The per capita freshwater consumption in Egypt is less than 13 % of the world's capita consumption.

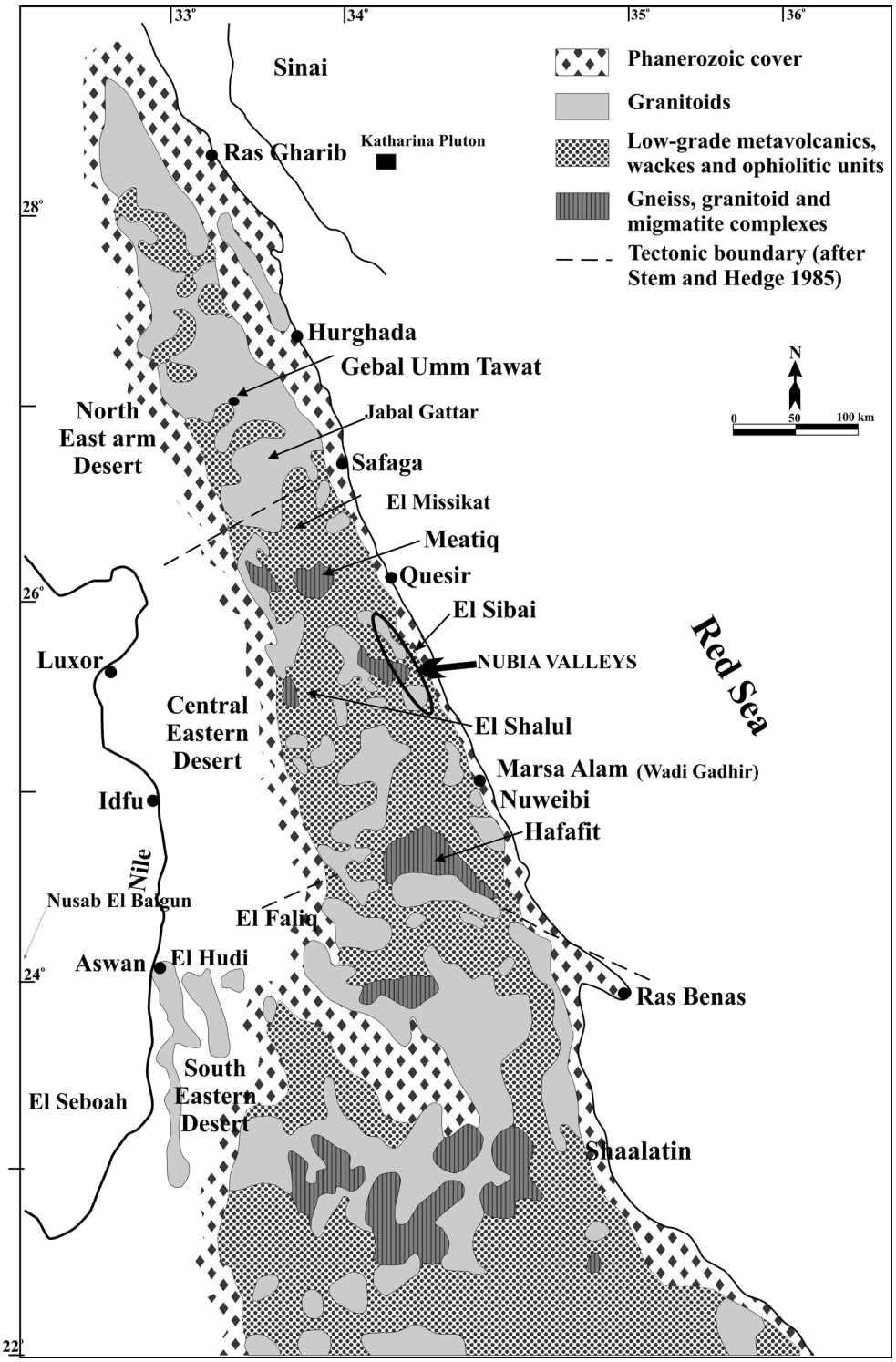

Fig. 7 Map showing the distribution of granites and associated rocks in the eastern desert region (Lundmark et al. 2012)

Further, Egypt suffers from uneven distribution of freshwater due to shortage in storage of the Nile river water. It has been projected that Egypt will face severe water shortage in future and may not be able to meet the demand for the growing population (Karameld and Mekhermar 2001). Like Saudi Arabia and other gulf countries, Egypt has to depend on desalination process to support the above demand of the current 82 million population with an annual growth of 1.6–3 % (Chandrasekharam et al. 2016). At present, 142 tera-Wh h of electricity that is being consumed is supported by oil- and gas-based power plants. The CO_2 emissions from the fossil fuels-based power plants are

Table 2 Uranium, thorium and potassium content and heat generated by certain the granites from south-western Egypt

	Sample no.	U (ppm)	Th (ppm)	K (%)	RHP ($\mu W\ m^{-3}$)	Heat Flow (mW/m^2)	Ref.
1	D163	5.0	27.0	4.2	3.5	75.4	1
2	D165	6.0	26.0	4.1	3.7	77.3	1
3	D82	6.0	23.0	4.2	3.5	75.2	1
4	D135	4.0	31.0	4.2	3.6	75.7	1
5	D97	10.0	40.0	3.9	5.7	97.0	1
6	D54	11.0	31.0	3.5	5.3	93.0	1
7	D59	9.0	30.0	3.7	4.7	87.3	1
8	D93	8.0	30.0	3.7	4.5	84.8	1
9	D43	9.0	36.0	3.6	5.1	91.4	1
10	D40	10.0	29.0	3.3	4.9	88.9	1
11	1.0	251.0	252.0	3.4	82.3	862.5	2
12	2.0	360.0	548.0	2.9	130.7	1346.9	2
13	3.0	230.0	414.0	3.1	88.0	920.2	2
14	4.0	373.0	571.0	2.6	135.6	1395.9	2
15	5.0	384.0	439.0	3.2	129.3	1333.5	2
16	6.0	240.0	432.0	3.6	91.9	958.9	2
17	10.0	2.0	5.0	3.0	1.1	51.4	3
18	11.0	8.0	13.0	3.1	3.2	72.4	3
19	12.0	7.0	17.0	2.8	3.2	72.4	3
20	17.0	9.0	15.0	3.2	3.7	76.5	3
21	19.0	13.0	24.0	3.5	5.3	93.3	3
22	3.0	17.0	31.0	2.7	6.8	107.7	3
23	6.0	14.0	33.0	2.8	6.1	101.4	3
24	40.0	6.0	22.0	3.4	3.4	73.8	3
25	41.0	9.0	30.0	2.9	4.7	86.6	3
26	43.0	13.0	29.0	3.2	5.6	96.4	3
27	46.0	7.0	23.0	3.5	3.7	77.2	3
28	48.0	8.0	27.0	3.0	4.2	82.0	3
29	23.0	5.0	17.0	2.7	2.7	67.2	3
30	26.0	7.0	18.0	2.9	3.3	73.2	3
31	32.0	4.0	13.0	2.7	2.2	61.8	3
32	33.0	6.0	16.0	2.8	2.9	69.1	3
33	34.0	2.0	7.0	1.9	1.2	51.7	3
34	36.0	4.0	13.0	2.6	2.2	61.7	3
35	38.0	5.0	15.0	3.1	2.6	66.1	3
36	39.0	3.0	10.0	2.9	1.7	57.4	3
37	1.0	6.0	22.0	4.3	3.5	74.7	4
38	2.0	4.0	17.0	4.2	2.6	66.0	4
39	3.0	12.0	30.0	3.4	5.5	94.7	4
40	4.0	13.0	34.0	4.1	6.1	100.8	4
41	5.0	10.0	27.0	4.0	4.8	88.2	4
42	6.0	10.0	36.0	4.6	5.5	94.9	4
43	7.0	14.0	50.0	4.9	7.5	115.1	4
44	8.0	34.0	22.0	4.6	10.7	146.9	4
45	9.0	25.0	26.0	3.7	8.6	125.7	4
46	10.0	14.0	20.0	4.1	5.4	93.7	4
47	11.0	26.0	22.0	4.0	8.6	125.8	4
48	1.0	7.0	13.3	3.4	3.0	70.3	5
49	2.0	6.6	8.0	0.3	2.3	62.7	5
50	3.0	16.9	33.8	0.1	6.7	106.8	5

Table 2 continued

	Sample no.	U (ppm)	Th (ppm)	K (%)	RHP (μW m^{-3})	Heat Flow (mW/m^2)	Ref.
51	4.0	18.5	24.4	2.3	6.7	106.6	5
52	5.0	14.1	18.3	1.6	5.0	90.3	5
53	7.0	10.7	21.1	3.8	4.6	85.7	5
54	AN2	38.3	14.4	3.8	11.2	151.9	5
55	AN1	64.0	26.2	3.3	18.6	225.7	5
56	1S	84.0	12.0	3.0	22.7	267.1	5
57	2S	86.0	15.0	3.3	23.5	274.6	5
58	3S	85.0	8.0	3.6	22.7	267.3	5
59	4S	85.0	9.0	4.1	22.9	268.5	5
60	5S	78.0	13.0	3.2	21.3	252.5	5
61	11.0	80.0	7.0	2.8	21.3	253.1	5
62	12.0	90.0	15.0	2.8	24.4	284.4	5
63	13.0	83.0	5.0	2.6	21.9	259.2	5
64	14.0	78.0	7.0	3.1	20.8	248.3	5
65	15.0	85.0	9.0	3.0	22.8	267.5	5
66	A1	225.0	25.0	4.6	60.0	640.0	5
67	A2	210.0	28.0	5.1	56.4	603.9	5
68	Nwb1	5.4	18.5	3.7	3.0	70.1	6
69	Nwb2	5.4	18.2	3.4	3.0	69.7	6
70	Nwb3	6.5	19.3	4.2	3.4	74.0	6
71	Nwb4	5.8	23.4	5.1	3.6	75.9	6
72	Nwb5	5.1	16.8	3.6	2.8	68.1	6
73	Nwb6	3.7	23.2	4.1	2.9	69.4	6
74	Nwb7	4.7	26.7	3.9	3.4	74.2	6
75	Nwb8	2.8	23.1	3.9	2.7	66.8	6
76	Nwb9	4.8	26.6	4.0	3.4	74.5	6

The heat flow is calculated assuming a 10-km-thick granite slab (source: 1: Katzir et al. 2007, 2: Saleh et al. 2014, 3: Emam et al. 2011, 4: Saleh 2006, 5: Raslan and El-Feky 2012, 6: Gaafar 2014)

about 204 million tonnes (Chandrasekharam et al. 2015). As described in "Present energy demand and CO_2 emissions", if Egypt adopts BAU or HEG strategy, it is going to only increase the CO_2 content. A renewable source mix will definitely curtail CO_2 emissions by half (Fig. 2) together with implementing energy efficiency policy in all the sectors by the country. In fact, the levelized cost of renewable energy projects given in Table 3 (Chandrasekharam et al. 2014) clearly indicates that geothermal energy sources have an edge over other renewables (Fig. 12). Even though the levelized cost of biomass is lower than other renewables, black carbon (BC) emissions from biomass are more harmful than the CO_2.

Wind energy that is extensively used in Egypt is generating about 550 MWe and expected to grow to 8760 MWe by 2022 (El Sobki et al. 2009). The New and Renewable Energy Association (NREA) is currently selling wind power at subsidized rate of 2.5 US cents/kWh (the actual cost, on an average, is 10 US cents/kWh) which is much below the generation cost itself. The American Wing Association fixed tariff for wind generated power at 6.5 US cents/kWh (average). Such kind of electricity tariff will not sustain on a long term and power this is detrimental to the power producers. But, wind energy cannot provide base-load electricity, and hence, a backup system is necessary that will apparently escalate the cost. Even if carbon credits are factored into the wind power tariff structure, the cost of power is not economical (Fig. 11).

Egypt has alternative sources to wind. The geothermal energy sources need to be considered as an energy source mix together with the wind and other renewables even though biomass has its own drawback. But in rural areas, this is the only energy source that supports life. The geothermal power plants operate at >90 % efficiency all the 365 days in a year. The life of geothermal power plant is greater than 30 years (e.g. the Larderello power plants is 100 years old). The payback period of geothermal power projects in 5 years unlike other sources that take far greater than 5 years. The rural areas will be highly benefited by mining the heat from these granites.

The estimated geothermal potential of Egypt is in the range of 95–221 $\times$ 10^6 kWh (Lashin 2012; Zaher et al.

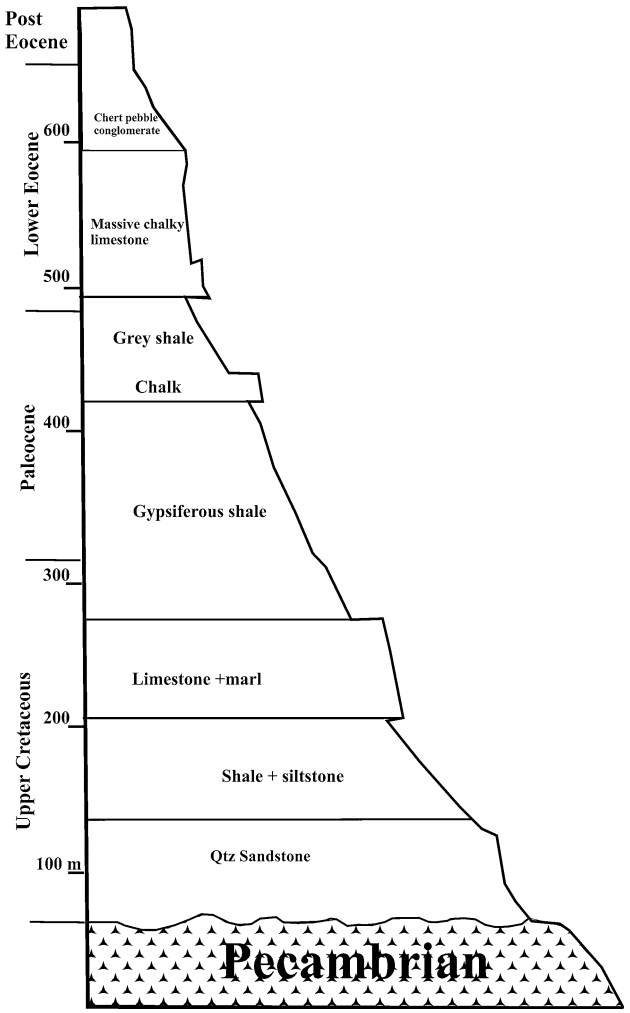

Fig. 8 Stratigraphic column around Qusier (see Fig. 7 for location) showing the sedimentary formations above the Precambrian basement (modified after Greene 1984)

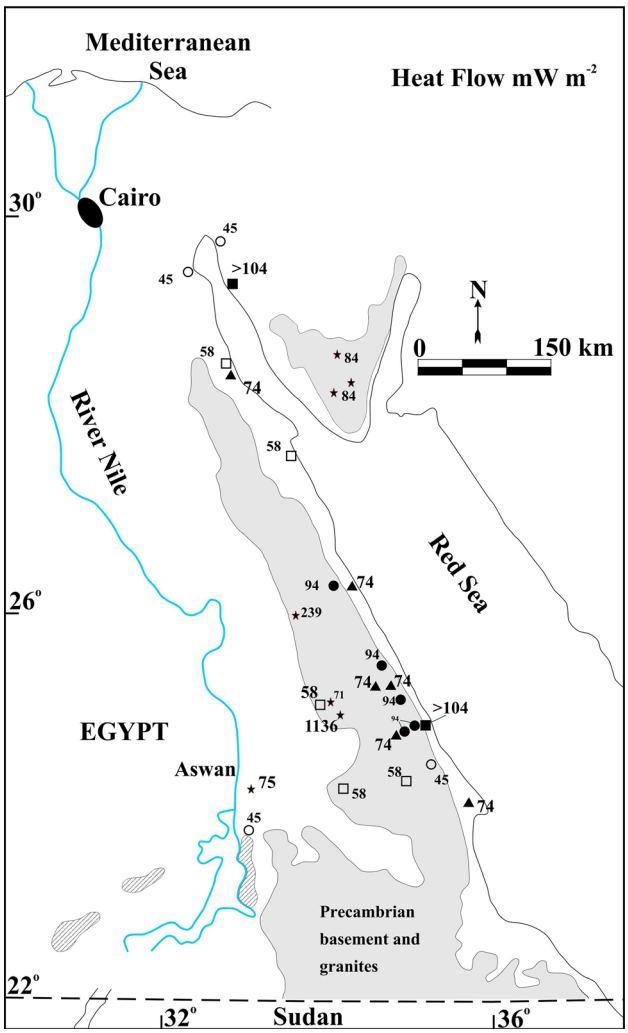

Fig. 9 Heat flow values over the eastern desert region (modified Morgan et al. 1985)

2012). In Egypt, the current electricity generation from oil is 25×10^9 kWh. If Egypt can tap 95×10^6 kWh from geothermal, then the country can save oil equivalent to the generation of the above amount of centricity that can be exported. In addition to hydrothermal resources, Egypt has substantial EGS sources locked up in the radiogenic granites described above (Figs. 9, 11; Table 2), similar to that present in the western Saudi Arabian shield (Chandrasekharam et al. 2015; Lashin et al. 2014). 1 km^3 of high heat-generating granite can generate 79×10^6 kWh (Somerville et al. 1994). For example, the El Faliq granite has a surface exposure of 95 km^2. Assuming that a reservoir is engineered in this granite between 2 and 3 km depth, about 7×10^9 kWh electricity can be generated. Thus, a substantial amount of electricity can be generated from all the radiogenic granites of eastern desert region. This is possible since in the next couple of years EGS technology will mature fully and countries can exploit such granites to be energy independent (MIT 2006). The technology to create fracture network in such granites is maturing (Baria et al. 2004; Hogarth et al 2013; Singh et al. 2015), and technology to circulate CO_2 instead of water for heat recovery from hot radiogenic granites is also maturing (Pruess 2006). These remote sites may not have a transmission network. But electricity generated from EGS sources can be supplied to the local communities through a local dedicated transmission network (for example oasis sites). The third option shown in Fig. 2 can be fully adopted by the country to save nearly 20 million tonnes of CO_2 by 2030.

The third option (Fig. 2) can help the country to enhance the gas exports from the current 17 billion cubic metres to 23 billion cubic metres by 2030. This will increase the country's GDP and make the country energy independent and food secured by 2030.

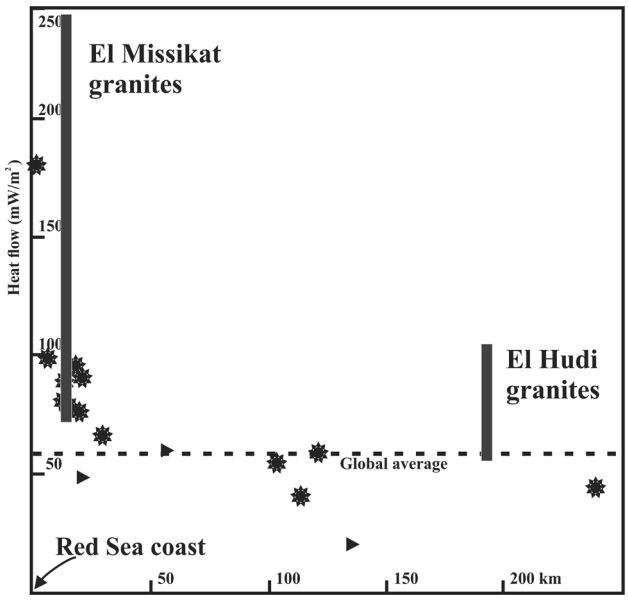

Fig. 10 Heat flow profile across the eastern desert (south of 26° latitude, Fig. 9), Egypt. Stars (granites) and triangles (sediments) were reported by Morgan et al. (1985). The heat flow values of El Hudi and El Missikat granites (Fig. 9; Table 2) are included to show the wide heat flow values across the desert

Table 3 US average levelized costs (2011 $/megawatthour) for plants entering service in 2018

	1	2	3	4	5	6
Geothermal	92	76	12	0.0	1	9.0
Biomass	83	53	14	42.3	1	11.1
Wind	34	70	13	0.0	3	8.7
Wind offshore	37	193	22	0.0	6	22.1
Solar PV[a]	25	130	10	0.0	4	14.4
Solar thermal	20	214	41	0.0	6	2.6
Hydro[b]	52	78	4	6.1	2	9.0

1 capacity factor, *2* levelized capital cost, *3* fixed O & M, *4* variable O & M, *5* transmission investment, *6* levelized cost US$c/kWh

[a] Costs are expressed in terms of net AC power available to the grid for the installed capacity

[b] As modelled, hydro is assumed to have seasonal storage so that it can be dispatched within a season, but overall operation is limited by resources available by site and season

About a decade, ago Egypt seriously considered nuclear option to generate freshwater through desalination process (Karameld and Mekhermar 2001). But now, the country has a safe option to generate freshwater through EGS

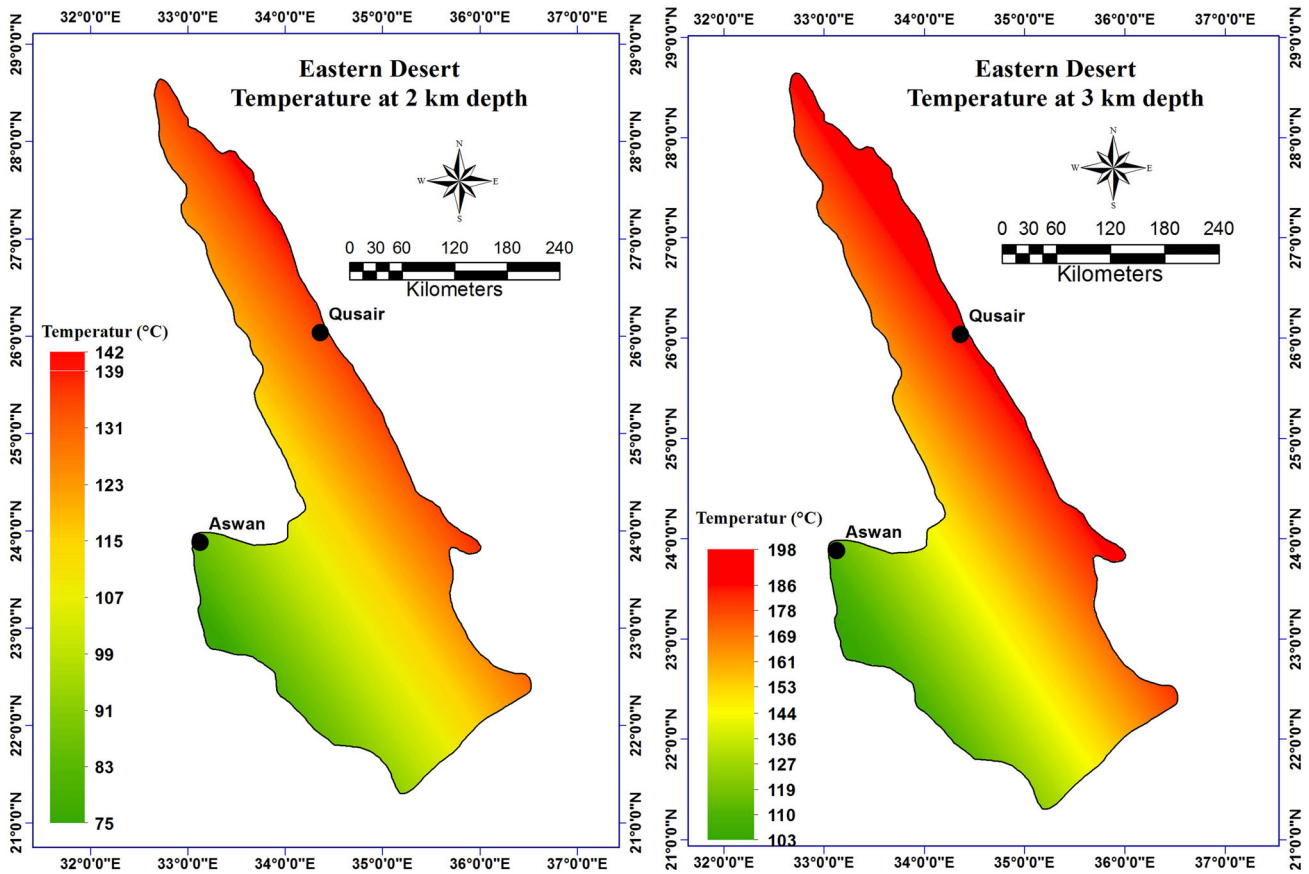

Fig. 11 Subsurface temperature at 2 ad 3 km depth, eastern desert Egypt

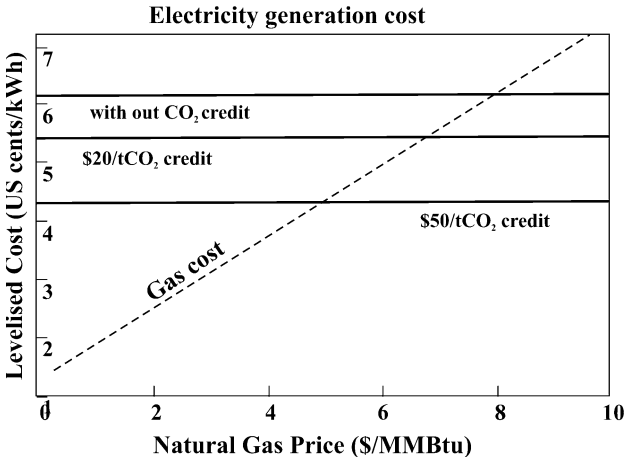

Fig. 12 Levelized cost of wind power with and without CO_2 subsidy compared to gas power (modified after El Sobki et al. 2009)

source to meet the freshwater demand from domestic, agricultural and industrial sectors. The current supply of 77 billion m^3 of freshwater can easily be enhanced using the energy locked up in these granites.

Even though Egypt has the largest oil and gas fields, the oil production has drastically declined in the recent past and the current production of 720,000 bbl/day is not able to meet the country's growing population which is currently at the rate of 3 % annually. Egypt's population is projected to grow to 108 million by 2025 from the current 87 million (Karameld and Mekhermar 2001).

To meet the energy demand, Egypt currently is importing oil to support tourism and manufacturing industries. Under the current scenario, Egypt needs energy mix to tone up its economy. Egypt has option to develop its EGS sources and save on the domestic oil and gas consumption and mitigate CO_2 emissions. Although wind energy is supporting part of the energy demand, this source cannot supply baseload electricity and cost subsidies on electricity generated through wind is will not sustain for a longer period and the cost of wind will exceed 12 US cents/kWh that is not economical on a long term basis ((El Sobki et al. 2009).

Conclusions

The current energy scenario of Egypt indicates that the oil and gas resources declining with the current production rate of 720,000 bbl/day. This amount may not be able to meet the country's future energy demand with population reaching 108 million by 2025. In addition to energy, demand for freshwater is growing due to uneven distribution of freshwater supply as a result of decline in surface flow of Nile River. However, Egypt has an option to mitigate future energy demand and freshwater supply by harnessing its huge geothermal resources locked up in its high radiogenic granites in the eastern desert region. Besides energy and freshwater supply, geothermal energy (energy source mix) will help the country to reduce CO_2 emissions there by controlling the CO_2 content in the atmosphere. Egypt should also implement energy efficient policy in sectors such as tourism, transport and agriculture. The levelized cost of renewable energy projects given in Table 3 clearly shows that geothermal energy has an advantage over other renewables. With the advancement of technology to create fracture pattern in granites at 2–3 km depths, and CO_2 being tested to extract heat from such high heat-generating granites, EGS projects will make Egypt energy, food and water secured country. Thus, geothermal energy in combination with other renewables motioned above can change the socio-economic status of the rural population and support the future population with energy and food security.

Acknowledgments The authors extend their sincere appreciation to the Deanship of Scientific Research at King Saud University for its funding of this research group No. (RG-1435-070). The corresponding author thanks the Director Indian Institute of Technology Bombay for providing the facilities for this work.

References

Abdalla FA, Scheytt T (2012) Hydrochemistry of surface water and groundwater from a fractured carbonate aquifer in the Helwan area, Egypt. J Earth Syst Sci 121:109–124

Baba A, Deniz O, Ozcan H, Erees SF, Cetiner SZ (2008) Geochemical and radionuclide profile of Tuzla geothermal field, Turkey. Environ Monit Assess 145:361–374

Baria R, Michelet S, Baumgärtner J, Dyer B, Gerard A, Nicholls J, Hettkamp T, Teza D, Soma N, Asanuma H (2004) Microseismic monitoring of the world largest potential HDR reservoir. In: Proceedings of the 29th workshop on geothermal reservoir engineering. Stanford University, California

Bentor YK (1985) The crustal evolution of the Arabo-Nubian Massif with special reference to the Sinai Peninsula. Precambr Res 28:1–74

Breger M, Bauernhofer A, Pelz K, Kloetzli U, Fritz H, Neumayr P (2002) A late Neoproterozoic magmatic core complex in the Eastern Desert of Egypt: emplacement of granitoids in a wrench-tectonic setting. Precambr Res 118:59–82

Cermak V, Huckenholz HG, Rybach L, Schmid R (1982) Radioactive heat generation in rocks. In: Hellwege K (ed) Landolt–Bornstein numerical data and functional relationships in science and technology. New series, group V. geophysics and space research, vol 1, physical properties of rocks, subvolume b. Springer, Berlin, Heidelberg, New York, pp 433–481

Chandrasekharam D, Lashin A, Al Arifi N (2014) CO_2 mitigation strategy through geothermal energy, Saudi Arabia. Renew Sustain Energy Rev 38:154–163

Chandrasekharam D, Lashin A, Al Arifi N, Al Bassam AA, Varun C (2015) Evolution of geothermal systems around the Red Sea. Environ Earth Sci 73:4215–4236

Chandrasekharam D, Lashin A, Al Arifi N, Al Bassam AM (2016) Red Sea geothermal provinces. CRC Press, UK, p 250 **(in press)**

Colletta B, Le Quellec P, Letouzey J, Moretti I (1988) Longitudinal evolution of the Suez rift structure (Egypt). Tectonophysics 153:221–233

de la Vega FF (2010) Impact of energy demand on Egypt's oil and natural gas reserves: current situation and perspectives to 2030. In: Sawin J, Mastny L (eds) "Egyptian–German joint committee on renewable energy, energy efficiency and environmental protection", Pub: Deutsche Gesellschaft für Technische Zusammenarbeit (GTZ) GmbH, pp 1–83

Eby GN (1992) Chemical subdivision of the A-type granitoids; petrogenetic and tectonic implications. Geology 20(7):641–644

El Ahmady Ibrahim M, El Hamed El Kalioby BA, Aly MG, El Tohamy AM, Watanabe K (2015) Altered granitic rocks, Nusab El Balgum Area, Southwestern Desert, Egypt: mineralogical and geochemical aspects of REEs. Ore Geol Rev 70:252–261

El Ramly MF, Akaad MK (1960) The basement complex in the central-eastern desert of Egypt between latitudes 24°30′ and 25°40N. Geol Surv Egypt 8:1–35

El Shaer HM (2010) Potential role of salt marshes in the Sabkhas of Egypt. In: Ozturk M, Boer B, Barth HJ, Breckle SW, Clusener-Godt M, Khan MA (eds) Sabkha ecosystems, volume III: Africa and Southern Europe, series for vegetation science, vol 46, pp 95–98

El Sobki M, Wooders P, Sherif Y (2009) Clean energy investment in developing countries: wind power in Egypt. International Institute for Sustainable Development (http://www.iisd.org), Trade, Investment and climate change series report, 54

Elsayed RAM, Assran HM, Elatta SAA (2014) Petrographic, radiometric and paleomagnetic studies for some alkaline rocks, south Nusab El Balgum mass complex, south western Egypt. Geomaterials 4:27–46

Emam A, Moghazy NM, El-Sherif AM (2011) Geochemistry, petrogenesis and radioactivity of El Hudi I-type younger granites, South Eastern Desert, Egypt. Arab J Geosci 4:863–878

Evans TR, Tammemagi HY (1974) Heat flow and heat production in north-east Africa. Earth Planet Sci Lett 23:349–356

Fritz H, Wallbrecher E, Khudeir AA, Abu El Ela F, Dallmeyer DR (1996) Formation of Neoproterozoic metamorphic core complexes during oblique convergence (Eastern Desert, Egypt). J Afr Earth Sc 23:311–329

Gaafar I (2014) Geophysical mapping, geochemical evidence and mineralogy for Nuweibi Rare Metal Albite granite, Eastern Desert, Egypt. Open J Geol 4:108–136

Gettings ME (1982) Heat flow measurements at shot points along the 1978 Saudi Arabian seismic deep refraction line, part 2: discussion and interpretation. USGS open file report, 82-794

Gettings ME, Showail A (1982) Heat flow measurements at shot points along the 197X Saudi Arabian seismic deep-refraction line, part I: results of the measurements, U.S. Geological Survey of open file report, 82-793, 98

Giggenbach WF (1988) Geothermal solute equilibria. Derivation of Na–K–Mg–Ca geoindicators. Geochim Cosmochim Acta 52:2749–2765

Girdler RW (1970) A review of Red Sea heat flow. Philos Trans R Soc Lond A 267:191–203

Greene DC (1984) Structural geology of the Qusier area, Red Sea cost, Egypt. Department of Geology and Geography contribution number 52, University of Massachusetts, USA, p 179

Hassan MA, Hashad AH (1990) Precambrian of Egypt. In: Said R (ed) The geology of Egypt. Balkema, Rotterdam, pp 201–248

Hogarth R, Holl H, McMahon A (2013) Flow testing results from Habanero EGS Project. In: Proceedings of the sixth annual Australian geothermal energy conference, 14–15 Nov 2013

Karameld A, Mekhermar S (2001) Sitting assessment of a water electricity cogeneration nuclear power plant in Egypt. Desalination 137:45–51

Katzir Y, Eyal M, Litvinovsky BA, Jahn BM, Zanvilevich AN, Valley JW, Beeri Y, Pelly I, Shimshilashvili E (2007) Petrogenesis of A-type granites and origin of vertical zoning in the Katharina pluton, Gebel Mussa (Mt. Moses) area, Sinai, Egypt. Lithos 95:208–228

Khalil A, Mubarak A, Kaseb S (2010) Road map for renewable energy research and development in Egypt. J Adv Res 1:29–38

Lachenbruch AH (1968) Preliminary geothermal model of the Sierra Nevada. J Geophys Res 73:6977–6989

Lashin A (2012) A preliminary study on the potential of the geothermal resources around the Gulf of Suez, Egypt. Arab J Geosci. doi:10.1007/s12517-012-0543-4

Lashin A, Chandrasekharam D, Al Arifi N, Al Bassam A, Chandrasekhar V (2014) Geothermal energy resources of wadi Al-Lith, Saudi Arabia. J Afr Earth Sci 97:357–367

Lundmark AM, Andresen A, Hassan MA, Augland LE, Boghdady GY (2012) Repeated magmatic pulses in the East African Orogen in the Eastern Desert, Egypt: an old idea supported by new evidence. Gondwana Res 22:227–237

MIT (2006) The future of geothermal energy—impact of enhanced geothermal systems (EGS) on the United States in the 21st Century. In: An assessment by an MIT led interdisciplinary panel. MIT—Massachusetts Institute of Technology, Cambridge, MA, p 358

Morgan P, Black'well DD, Fanis TG, Boulos FK, Salib PG (1976) Preliminary temperature gradient and heat flow values for northern Egypt and the Gulf of Suez from oil well data. In: Proceedings international congress on thermal waters. Geothermal energy and volcanism of Mediterranean area. Geothermal energy, vol 1, pp 424–438

Morgan P, Blackwell DD, Farris JC, Boulos FK, Salib PG (1977) Preliminary geothermal gradient and heat flow values for northern Egypt and the Gulf of Suez from oil well data. In: Proceedings of the international congress of thermal waters, geothermal energy and vulcanism of the Mediterranean area, vol I. National Technical University, Athens, Greece, pp 424–438

Morgan P, Boulos FK, Hennin SF, El-Sherif AA, EI-Saycd AA, Basta NZ, Melek YS (1981) Geophysical investigations of a geothermal anomaly at Wadi Ghadir, eastern Egypt. InL Proceedings of the first annual meeting Egyptian Geophysical Society, Cairo, 28 Sept, vol 29, p 17

Morgan P, Boulos FK, Swanberg CA (1983) Regional geothermal exploration in Egypt. Geophys Prospect 31:361–376

Morgan P, Boulos FK, Hennin SF, El-Sherif AA, El-Syed AA, Basta NZ, Melek YS (1985) Heat flow in eastern Egypt: the thermal signature of a continental breakup. J Geodyn 4:107–131

Moussa EMM, Stern R, Manton WI, Ali KA (2008) SHRIMP zircon dating and Sm/Nd isotopic investigations of Neoproterozoic granitoids, Eastern Desert, Egypt. Precambr Res 160:341–356. doi:10.1016/j.precamres.2007.08.006

Nagy RM, Ghuma MA, Rogers JJ (1976) A crustal suture and lineaments in North Africa. Tectonophysics 31:67–72

Patton TL, Moustafa AR, Nelson RA, Abdine AS (1994) Tectonic evolution and structural setting of the Suez rift. In: Landon SM (ed) Interior rift basins, vol 58. American Association of Petroleum Geologists Mere, pp 9–55

Perrin M, Saleh A, Valdivia LA (2009) Cenozoic and Mesozoic basalt from Egypt: a preliminary survey. Earth Planets Space 61:51–60

Piper AM (1953) A graphic procedure in the geochemical interpretation of water analyses. USGS groundwater note, p 12

Pruess K (2006) Enhanced geothermal systems (EGS) using CO2 as working fluid—a novel approach for generating renewable energy with simultaneous sequestration of carbon. Geothermics 35:351–367

Raslan MF, El-Feky MG (2012) Radioactivity and mineralogy of the altered granites of the Wadi Ghadir shear zone, South Eastern Desert, Egypt. Chin J Geochem 31:030–040

Rybach L (1976) Radioactive heat production: a physical property determined by the chemistry. In: Strens RGI (ed) The physical and chemistry of minerals and rocks. Wiley-Interscience Publication, New York, pp 245–276

Saleh GM (2006) Uranium mineralization in the muscovite-rich granites of the Shalatin region, Southeastern desert, Egypt. Chin J Geochem 25:1–15

Saleh S, Jahr T, Jentzsch G, Saleh A, Ashour NMA (2006) Crustal evaluation of the northern Red Sea rift and Gulf of Suez, Egypt from geophysical data: 3-dimensional modelling. J Afr Earth Sci 45:257–278

Saleh GM, Mostafa DA, Darwish ME, Salem IA (2014) Gabal El Faliq Granitoid rocks of the Southeastern Desert, Egypt: geochemical constraints, mineralization and spectrometric prospecting. Stand Glob J Geol Explor Res 1(1):009–026

Schandelmeier H, Pudlo D (1990) The Central-African fault zone in Sudan—a possible continental transform fault. Berl Geowiss Abh 120-A:31–44

Singh B, Ranjith PG, Chandrasekharam D, Viete HK, Singh A, Lashin N Al, Al Arifi N (2015) Thermo-mechanical properties of Bundelkhand Granite near Jhansi, India. Geomecha Geophy Geoener Geores. doi:10.1007/s40948-015-0005-z

Somerville M, Wyborn D, Chopra P, Rahman S, Don Estrella, Theo Van der Meulen (1994) Hot dry rock feasibility study. Energy research and development corporation, Australia, p 170 **(unpublished report)**

Stern RJ (1985) The Najd Fault System, Saudi Arabia and Egypt: a late Precambrian rift-related transform system? Tectonics 4:497–511

Stern RJ (1994) Arc assembly and continental collision in the Neoproterozoic East African Orogen-Implications for the consolidation of Gondwanaland. Earth Planet Sci Ann Rev 22:319–351

Stern RJ, Johnson P (2010) Continental lithosphere of the Arabian Plate. A geologic, petrologic, and geophysical synthesis. Earth Sci Rev 101:29–67

Stern RJ, Gottfried D, Hedge CE (1984) Late Precambrian rifting and crustal evolution in the northeast Desert of Egypt. Geology 12:168–172

Swanberg CA, Morgan P, Boulos FK (1983) Geothermal potential of Egypt. Tectonophy 96:77–94

Vernekar AD (1975) A calculation of normal temperature at the Earth's surface. J Atmos Sci 32:2067–2081

Zaher MA, Saibi H, El-Nouby M, Ghamry E, Ehara S (2011) A preliminary regional geothermal assessment of the Gulf of Suez, Egypt. J Afr Earth Sci 60:117–132

Zaher MA, Saibi H, Nishijim J, Fujimitsu Y, Mesbah H, Ehara S (2012) Exploration and assessment of the geothermal resources in the Hammam Faraun hot springs, Sinai Peninsula, Egypt. J Asian Erth Sci 45:256–267